Vol. 36, No. 2 (2014) 211-219

Tribology in Industry

www.tribology.fink.rs

RESEARCH

Analysis of a Rough Elliptic Bore Journal Bearing using Expectancy Model of Roughness Characterization

P.C. Mishra[a]

[a] *Green Engine Technology Center, School of Mechanical Engineering, KIIT University, Bhubaneswar, India.*

Keywords:

Elliptic bore
Journal bearing
Stochastic model
Friction
Flow-in
Side leakage

Corresponding author:

Prakash Chandra Mishra
School of Mechanical Engineering
KIIT University ,Bhubaneswar, India
E-mail: pmishrafme@kiit.ac.in

A B S T R A C T

Performance characteristics of a rough elliptic bore journal bearing are studied. The bearing bore of isotropic roughness orientation is characterized by stochastic function and the film geometry is quantified to elliptic shape. There after the Reynolds equation and energy equation are descretized for pressure and temperature respectively. A finite difference model is developed to evaluate hydrodynamic pressure and oil temperature. Solution to this model is done using effective influence Newton-Raphson method. Performance parameters such as load bearing ability, friction, flow-in and side leakages are computed and discussed.

1. INTRODUCTION

Hydrodynamic journal bearings are most widely used in engines and power plants to support rotating shafts. Such bearing simply consists of rotating journal inside the bore of a sleeve. Constant entraining motion of lubricant into the converging and diverging conjunction of journal bearing happens due to rotation of shaft. The lubricant develops hydrodynamic reaction due to its inherent rheological properties and maintains separation between the static bore and the rotating journal. Theoretically bearing bore is assumed circular and smooth. But due to vibration of tools and jobs or due to eccentric positioning of tools with the job axis during machining, bearing bore actually becomes oval. Roughness is also produced due to tool profile roughness. While, evaluating the performance parameters, such irregularities must be addressed in the computation.

Mathematical computation of journal bearing parameters was first made in 1950s. Standard plots of different parameters like Summerfield number, coefficient of friction, power loss variable, minimum film thickness, position of minimum and maximum film thickness and pressure, flow variable, film temperature rise and viscosity variations were plotted for the requirement of field engineers [1].

Sometimes the bearing is subjected to load, which may act in any arbitrary direction [2]. Also, the partial journal bearings (150 ^{0}, 100 ^{0}, 75 ^{0}) are used for specific purposes. Hence

calculation for performance parameters of non-centrally loaded partially grooved multi-lobe bearings were done for entire attitude and load angle in case of short, long and finite journal bearing. Often, it is more appropriate to assume the bearing bore to be slightly irregular because of manufacturing tolerance. Elliptic bore shape is exact to real practice [3]. The nature of hydrodynamic action, the effect of load angle and attitude angle on bearing performance for various degree of ellipticity are worth discussing.

Though journal bearing is fluid film bearing, the bore roughness affects the flow pattern due to which the performance parameters are modified. Film that is developed in a rough surface can be quantified using a stochastic function [4]. The Reynolds equation for such rough journal bearing can be modified using the expectancy operators. Such operators are different for different rough orientation. Similar type stochastic model of roughness [4] are suitable to study the effect of surface texture on hydrodynamic lubrication of dynamically loaded journal bearing [5]. Rough porous bearing are subjected to slip condition while in operation [6]. The effect of slip velocity on hydrodynamic action can be modeled using stochastic theory. The load carrying capacity and the friction decreases with velocity slip. Hence the combined effect of surface roughness pattern and the non-Newtonian rheology on performance of dynamically loaded journal bearing is significant [7]. Rough contiguous surface develops more hydrodynamic pressure than smooth ones. The surface topography and orientation affects the EHL (Elasto hydrodynamic lubrication) characteristics [8].

Temperature rise in lubricant film occurs due to rapid shear of lubricant layer. The hydrodynamic action is affected due to thermal effect. Such temperature rise for a non-Newtonian lubricant can be better estimated using power law model [9]. The temperature profile [10] of elliptic journal bearing due to thermal effect shows different trends than circular one. The performance parameters for different eccentricity and non-circularity value show the clear difference [11]. The misaligned journal [12] and its dynamic stability [13] also affect the performance to a significant level due to roughness and non-circularity. The tribological principles have wide application [14], in which the sliding contacts are modeled for performance during high load and high speed application.

From the available literatures, it is understood that few of them are more inclined to roughness analysis and others are to thermal effects. A combined study of roughness and thermal effect will be a better contribution to elliptic journal bearing analysis and hence is the objective of this paper.

2. THEORY

In the static state a journal rests on the bearing. When the journal starts rotating, there develops the hydrodynamic action that maintains separation between the journal and the bore and develops hydrodynamic action as shown in the Fig. 1.

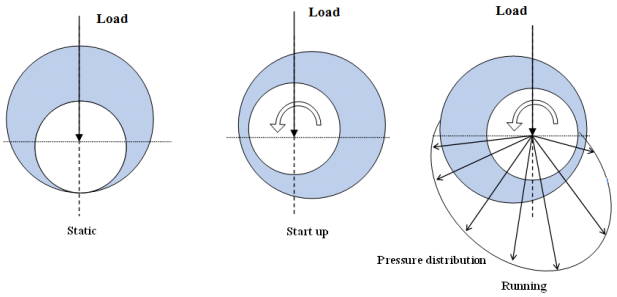

Fig. 1. Mechanism of journal bearing pressure development.

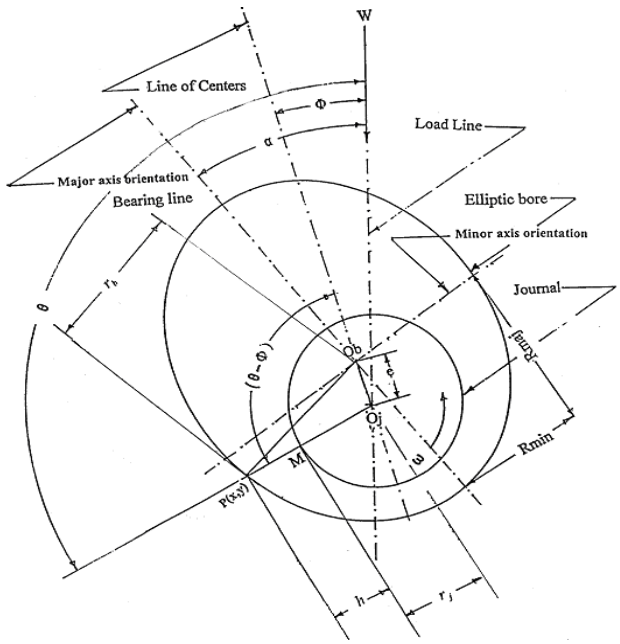

Fig. 2. Elliptic bore bearing and associated geometry as per Mishra et al [10].

From observation, it is found that journal bearing operates in fully flooded lubrication with film thickness of 5-50 μm. Hence, it is termed as bearing of infinite life.

In case of a journal bearing with an elliptic bore, there occurs two conjunctions for which two pressure bumps are developed. The expression for film thickness in this case is given in Eq. (1).

$$h = \begin{Bmatrix} R_{\min}\sin^2(\theta-\alpha)+R_{maj}\cos^2(\theta-\alpha) \\ -r_j+e\cos(\theta-\phi) \end{Bmatrix} \quad (1)$$

where,

$$\Psi = \frac{c}{R_{\min}} and \in = \frac{e}{c}$$

and,

$$G = \frac{(\delta-1)}{\Psi}, \delta = \frac{R_{maj}}{R_{\min}}$$

Therefore, the non-dimensional film thickness of an elliptic bore bearing will be as per Eq.(2):

$$H = 1 + G\cos^2(\theta-\alpha) + \in \cos(\theta-\phi) \quad (2)$$

The non-circularity G is the ovality/ellipticity of the bore. Its value affects greatly to the fluid film pressure. The 'α' is the angle of inclination of major axis with the load line. Similarly, φ is the attitude angle of the bearing.

2.1 Roughness Characterization of the bore

Fluid film thickness including surface roughness is considered as a stochastic process [4]. The fluid film geometry is split up in to two parts, namely; nominal film thickness which measures large-scale variation including any long wavelength disturbance and the part due to roughness measured from the nominal level.

Let h_n = nominal film thickness

and

h_s = Random/stochastic film thickness

The total film thickness is:

$$h = h_n + h_s \quad (3)$$

where,

$$h_n = c\times\left(1+G\cos^2\theta+\in\cos\theta\right) \quad (4)$$

and

$$h_s = f(\theta, z, \xi) \quad (5)$$

The structure of rough surface is a random variable represented by ξ.

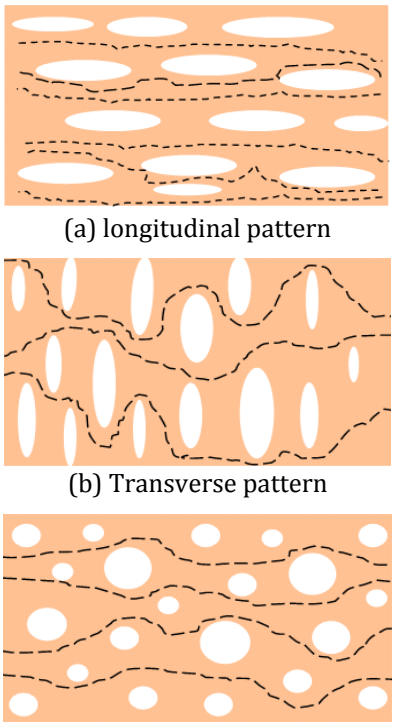

(a) longitudinal pattern

(b) Transverse pattern

(c) Isotropic pattern

Fig. 3. Flow pattern due to different roughness pattern of bore surface.

In this case the bore is considered rough and the shaft is smooth. The roughnesses are basically of three patterns, such as Longitudinal, transverse and isotropic. It is shown in the Fig. 3. Longitudinal pattern offers less resistance to flow. Transverse roughness offers more resistance to flow and better for pressure development for sealing devices, while isotropic roughness are equally good for lubricant flow and hydrodynamic action. The Reynolds equation for a rough elliptic bore with isotropic orientation is given as:

$$\frac{\partial}{\partial x}E\left(H^3\frac{\partial P}{\partial x}\right)+\frac{\partial}{\partial z}E\left(H^3\frac{\partial P}{\partial z}\right)=6\eta u\frac{\partial}{\partial x}E(H) \quad (6)$$

where,

$$E(x)=\int_{-\infty}^{\infty}xf(x)dx \quad (7)$$

$E(x)$ is the Expectancy operator and f (x)= probability density of stochastic variables.

The Eq (7) can be rewritten as:

$$\frac{\partial}{\partial x}\left(\frac{\partial P}{\partial x}\Psi_1(H)\right)+\frac{\partial}{\partial z}\left(\frac{\partial P}{\partial z}\Psi_2(H)\right)=6\eta u\frac{\partial}{\partial x}\Psi_3(H) \quad (8)$$

where,

$\Psi_1(H), \Psi_2(H) and \Psi_3(H)$ for isotropic roughness are given as:

$$\Psi_1 = E\left(H^3\right), \Psi_2 = E\left(H^3\right) and\ \Psi_3 = E\left(\frac{1}{H}\right)$$

and,

$$E\left(H^3\right) = H^3 + \frac{HY^2}{3}$$

$$E\left(\frac{1}{H}\right) = \frac{35}{37Y^7}\left\{\begin{matrix} 6\left(Y^2 - H^2\right)\log\frac{H+Y}{H-Y} + \\ \frac{2}{15}HY\left(15H^4 - 40Y^2H^2 + 33Y^4\right)\end{matrix}\right\}$$

The Y is the roughness factor with value of 0.1 or 0.2. The value 0.1 means 10% of the surface is having roughness. Similarly, 0.2 value represents 20% of the surface contains the defined roughness height.

2.2 Flow-in to the bearing

Flow-in is the amount of lubricant entered into the conjuction. The non-dimensional form of its intensity is given as:

$$q_{in} = \pi\frac{c}{R}\left(\frac{E\left(H_{i,j}\right)}{2} - \frac{1}{24}E\left(H_{i,j}{}^3\right).\frac{P_{i+1,j} - P_{i,j}}{\Delta\theta}\right) \quad (9)$$

and,

$$Q_{in} = \int\int q_{in} d\theta dZ$$

The Q_{in} is calculated by integrating the q_{in} over the unwrapped bearing area.

2.3 Side leakage from the bearing

The leakage flow Q_s out of the bearing is as follows:

$$q_s = -\frac{\pi}{12}.E\left(H_{i,j}^3\right).\frac{P_{i,j+1} - P_{i,j}}{\Delta Z} \quad (10)$$

$$Q_s = \int\int q_s d\theta dZ$$

and the Q_s calculated by integrating the q_s over the bearing area.

2.4 Temperature rise due to fluid friction

The rapid shear of the multi layer lubricant film and the friction between the relatively moving surfaces causes the temperature rise in the interface of lubricant. Heat generated out of this rubbing phenomenon is transferred by conduction to the moving shaft and the stationary bore (though conduction through shaft is very less compare to that through bore due to rapid change of position in the former case). Heat generated in side the bearing is also transferred by convection of lubricant flow. Part of the heat is also radiated. The rise in temperature and development of variable isotherm lines cause the viscosity variation in side a passive film. This variable viscosity causes the pressure to drop more in comparison to isothermal case. The increase in temperature causes decrease in viscosity as per following relation of thermal degradation.

$$\eta^* = \frac{\eta}{\eta_0} = e^{-\beta_{th}(T - T_0)} \quad (11)$$

where,

η^* = Non dimensional viscosity

$\eta =$ Viscosity consistency at temperature T

$\eta_0 =$ Viscosity consistency at temperature T_0

β_{th} = Viscosity temperature index

The thermal behavior of a bearing system affects the pressure and subsequently the load carrying capacity and other performance parameters.

Journal bearing is fluid film bearing. There is no solid-solid interaction because of full fluid film. Hence, the only source of heat generation is the frictional heat generated out of rapid shear of lubricant layers. The temperature of generated heat is obtained using power law model [9].

$$A\frac{\partial\lambda}{\partial\theta} + B\left(\frac{D}{L}\right)\frac{\partial\lambda}{\partial Z} = \alpha\frac{\eta^*}{H^2}\left(E + F\right) \quad (12)$$

where,

$$A = \frac{1}{2} - \frac{1}{12}\left(\frac{H^2}{e^{-\lambda}}\frac{\partial P}{\partial\theta}\right)$$

and,

$$B = -\frac{1}{12}\left(\frac{D}{L}\right)\left(\frac{H^2}{e^{-\lambda}}\frac{\partial P}{\partial Z}\right)$$

further,

$$E = 1 + \frac{1}{12}\frac{H^4}{e^{-2\lambda}}\left(\frac{\partial P}{\partial\theta}\right)^2$$

and,

$$F = \frac{1}{12}\left(\frac{H}{\beta_{th}e^{-\hat{\lambda}}}\right)^2\left(\frac{\partial P}{\partial Z}\right)^2$$

The temperature in this analysis is computed using the non-dimensional temperature expression derived by Mishra et al [10] and is given in Eq. (13).

$$\hat{\lambda} = \frac{\left[\frac{1}{2}\frac{\partial\hat{\lambda}}{\partial\theta} - \left\{\frac{30}{12}H^2\left(\frac{\partial P}{\partial\theta}\right)^2 + \frac{30}{12\beta_{th}^2}H^2\left(\frac{\partial P}{\partial Z}\right)^2\right\}\right] - \left[\left\{\frac{1}{12}H^2\frac{\partial P}{\partial\theta}\frac{\partial\hat{\lambda}}{\partial\theta} + \frac{1}{12\beta_{th}^2}H^2\frac{\partial P}{\partial Z}\frac{\partial\hat{\lambda}}{\partial Z}\right\} + \frac{30}{H^2}\right]}{\left[\left\{\frac{1}{12}H^2\frac{\partial P}{\partial\theta}\frac{\partial\hat{\lambda}}{\partial\theta} + \frac{1}{12\beta_{th}^2}H^2\frac{\partial P}{\partial Z}\frac{\partial\hat{\lambda}}{\partial Z}\right\} - \frac{60}{H^2}\right]} \quad (13)$$

The generated heat is transferred to the bush and to the shaft. Therefore the heat generated equal to the sum of the heat transferred to the shaft and that transferred to the bush.

2.5 Method of solution

The objective of this model is to evaluate the load bearing ability, friction force, flow-in and side leakage of the elliptic bore bearing and to develop the correlation between them. The steps involved in this computation are given as follows:

- At, first the entire bearing surface is unwrapped and a grid is formed with 90 numbers of nodes in direction of rotation and 16 numbers of nodes in direction of side leakage. The grid elements are near to square shape.
- Solution of Reynolds equation using a low relaxation method of pressure convergence as stated in Eq. (14). It includes the finite difference method to desretize the Reynold equation for pressure and to iterate the error of computed pressure based on error criteria given in Eq. (15).
- The flow chart for computation is given in Fig. 4. It presents the computational steps as first to evaluate the isothermal pressure and then the temperature rise in lubricant. Finally, to compute thermal pressure.
- The hydrodynamic pressure is integrated to calculate load capacity. The shear stress is integrated to calculate friction.
- Finally, the intensity of flow-in and that of side leakage are integrated over area to obtain total flow-in and total side leakage respectively.

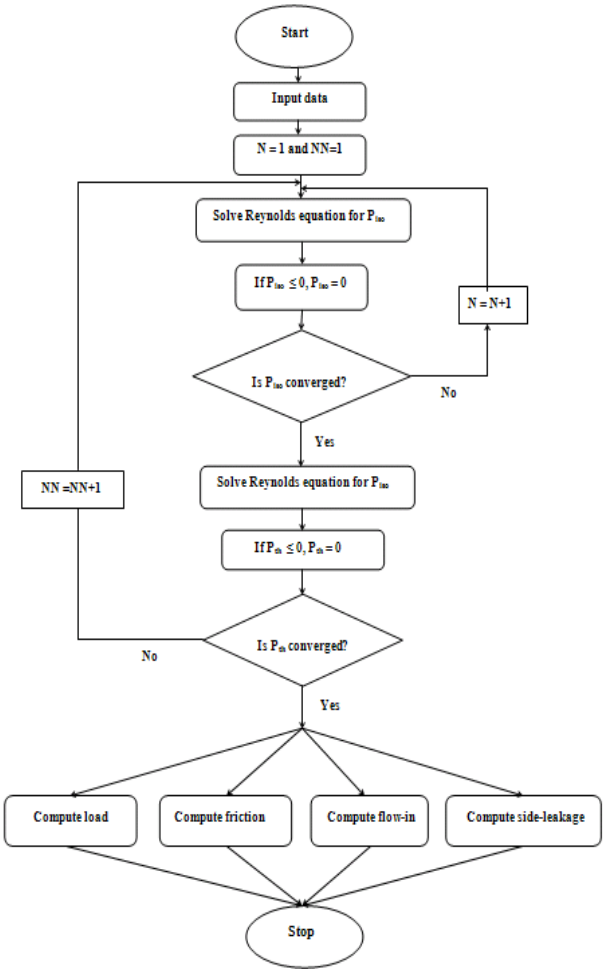

Fig. 4. Flow chart for computation.

$$P_{i,j}^K = P_{i,j}^K + orf.\left(P_{i,j}^{K+1} - P_{i,j}^K\right) \quad (14)$$

$$Error_{P_{th}} = \frac{\sum_i^m\sum_j^n\left|P_{iso}^{K+1} - P_{iso}^K\right|}{\sum_i^m\sum_j^n P_{iso}^K} \le 0.02 \quad (15)$$

$$Error_{P_{th}} = \frac{\sum_i^m\sum_j^n\left|P_{th}^{K+1} - P_{th}^K\right|}{\sum_i^m\sum_j^n P_{th}^K} \le 0.02 \quad (16)$$

$$Error_{\hat{\lambda}} = \frac{\sum_i^m\sum_j^n\left|\hat{\lambda}^{K+1} - \hat{\lambda}^K\right|}{\sum_i^m\sum_j^n \hat{\lambda}^K} \le 0.02 \quad (17)$$

Grid independent test is carried out for 90x16, 135x24 and 180x32 node combination. There is less than 5 % deviation in the results.

3. RESULT AND DISCUSSIONS

The gap between an elliptic bore and a circular shaft develops two conjunctions. Hence two pressure bumps are formed due to hydrodynamic action as given in figure5. A dynamic bearing with some degree of non-circularity/ ellipticity are found to be more stable because of hydrodynamic pressure in more contact area. The Fig. 6 represents comparison of bearing pressure due to isothermal consideration with that due to thermal consideration. The thermal case shows less pressure than as the temperature rise reduces the dynamic viscosity.

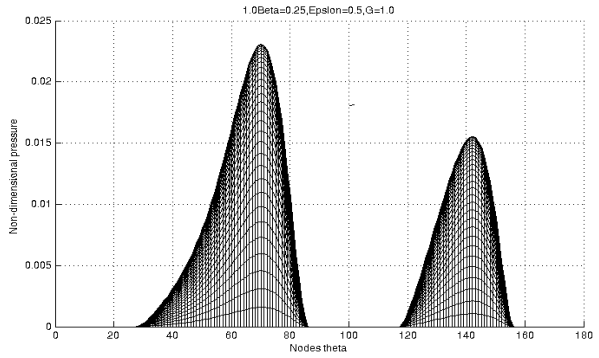

Fig. 5. Elliptic bore bearing pressure profile $(G=1.0, \beta=0.25, \in=0.5)$.

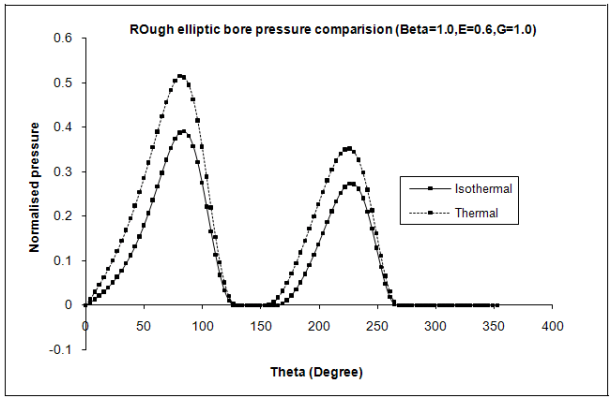

Fig. 6. Thermal and isothermal pressure comparison $(G=1.0, \beta=1.0, \in=0.6)$.

There is around 20 % decrease in highest pressure in the primary pressure profile and near to 15 % in secondary profile due to thermal consideration. The rise in temperature reduces the viscosity, for which the ability of lubricant film to develop hydrodynamic pressure reduces. The Fig. 7 shows the variation of temperature along the entraining direction of a finite journal bearing (β =1). It is difficult to observe the definite trends due to combined effect of non-circularity and eccentricity. But for the case of (G=1.0 and ϵ=0.6), the temperature rise is highest among all cases. The lowest being (G=1.5 and ϵ=0.6).

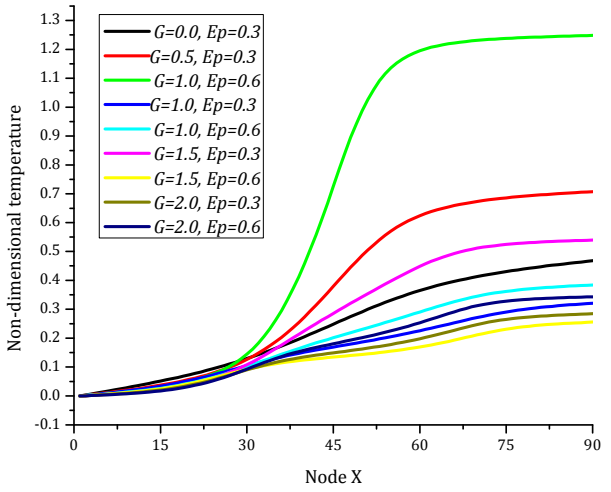

Fig. 7. Temperature variation along circumference with various eccentricity and non-circularity.

As the temperature rise affect hydrodynamic performance, it is more reliable to study the temperature distribution on the whole surface to identify the location of highest temperature rise. Contour mapping is the most suitable method to study the isotherms. Figure 8 to Fig. 11 represent the contour of temperature for various value of noncircularity. The temperature is higher in the core region than in the periphery of. It decreases with increase value of non-circularity. The highest non-dimensional temperature is in the range of $(1.16<\lambda<1.03)$ for $(0.3<G<3)$.

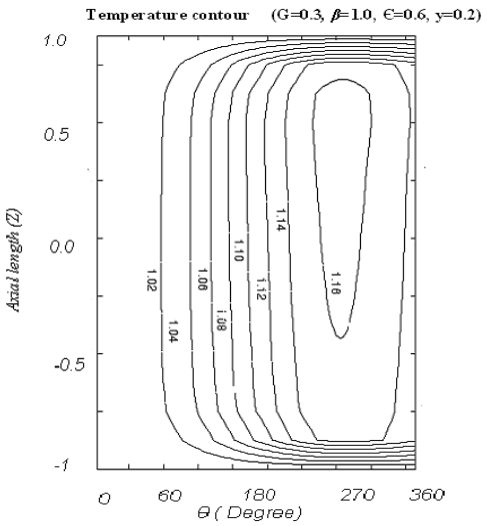

Fig. 8. Temperature contour $(G=0.3, \beta=1.0, \in=0.6, Y=0.2)$

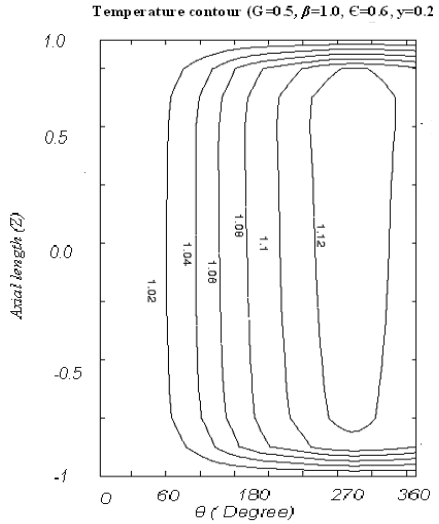

Fig. 9. Temperature contour
$(G = 0.5, \beta = 1.0, \in = 0.6, Y = 0.2)$

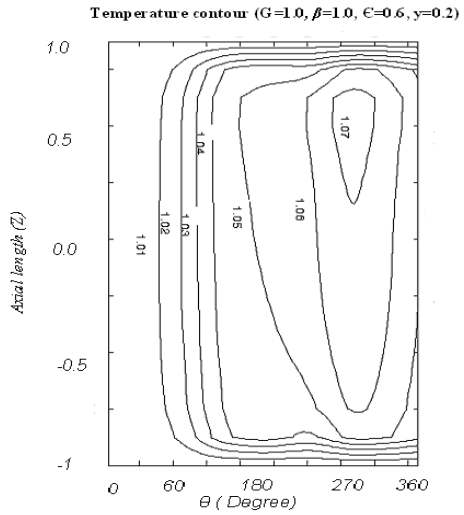

Fig. 10. Temperature contour
$(G = 1.0, \beta = 1.0, \in = 0.6, Y = 0.2)$

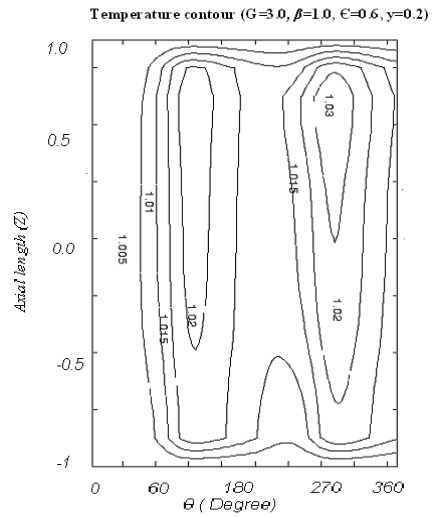

Fig. 11. Temperature contour
$(G = 3.0, \beta = 1.0, \in = 0.6, Y = 0.2)$

The increase of non-circularity beyond G=1.0 develops multiple regions with higher isotherms, but the highest temperature becomes lesser in comparison to bearing bore with lesser non-circularity value.

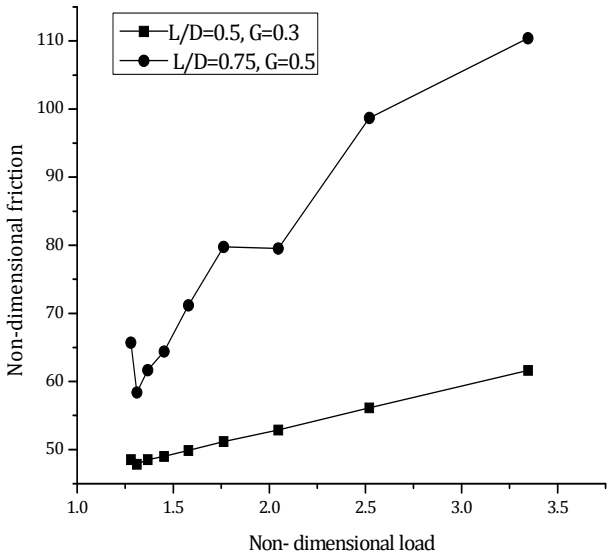

Fig. 12. Load and friction curve.

The Fig. 12 represents the load and friction inter-relationship for two different non-circularity values. For increasing load value, the friction increases. For higher non-circularity value, this trend is above the lower ones. The Fig. 13 represents the flow-in and side leakages inter-relationship. The bearing with roughness (*Y=0.1*) has more side leakage than that of smooth bearing. The Fig. 14 shows the graph of flow-in with friction. The friction is most in case of long bearing and least in case of short bearing.

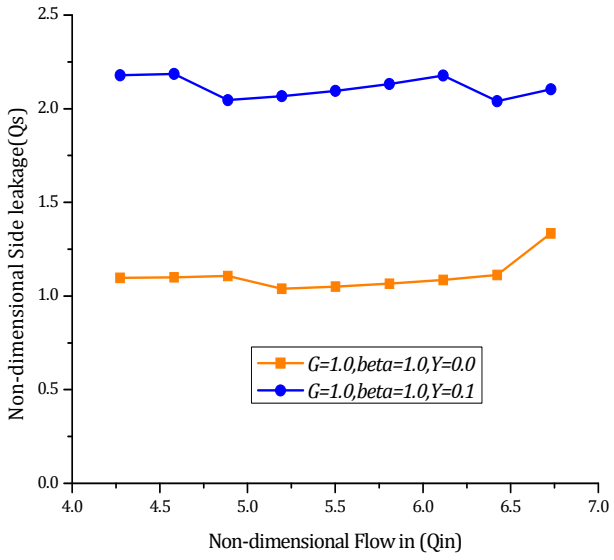

Fig. 13. Flow-in vs side leakage curve.

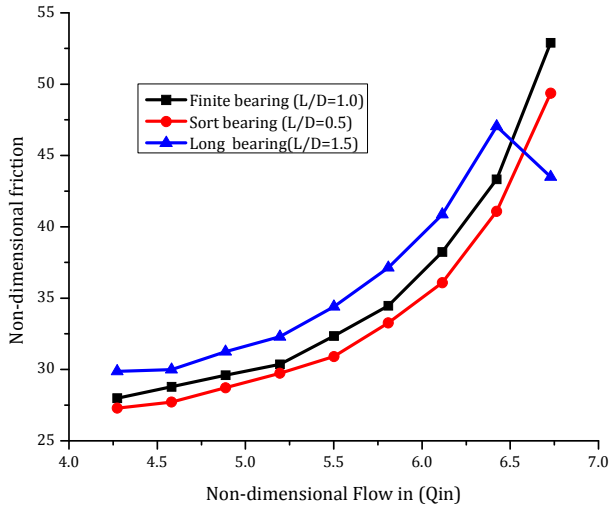

Fig. 14. Friction vs. Flow-in curve.

4. CONCLUSION

An elliptic bore bearing with non-circularity (0< G < 3.0) and isotropic roughness (Y= 0.1, Y= 0.2) is modeled for performance parameters. Parameters like hydrodynamic pressure, temperature rise, load capacity, friction, flow-in and side leakage are studied through plots.

Acknowledgement

We are very much thankful to the All India Council for Technical Education and Training (AICTE), New Delhi for funding this research. The funding of AICTE through RPS grant-in-aid to carry out our research project entitled "Advanced Engine Technology for Sustainable Development of Automotive Industry" is here acknowledged.

REFERENCES

[1] J. Boyd, A. Raimondi: *Applying bearing theory to the analysis and design of journal bearing –I & II,* ASME journal of applied mechanics, pp. 298-361, 1951.

[2] O. Pinkus: *Solution of Reynolds equation for Arbitrarily loaded Journal bearing,* Journal of Fluids Engineering, Vol. 83, No. 2, pp. 145-152, 1961.

[3] W.A. Crosby: *An Investigation of Performance of Journal Bearings with slightly irregular bore,* Tribol. Int., Vol. 25, No. 3, pp. 199-204, 1992.

[4] H. Christensen, K. Tonder: *The Hydrodynamic Lubrication of Rough Journal Bearings*, Journal of Lubrication Technol., Vol. 95, No. 2, pp. 166-172, 1973.

[5] I. Cheng: *Linear Stability of Short Journal Bearings with consideration of Flow Rheology and Surface Roughness,* Tribol. Int., Vol. 34, No. 8, pp. 507- 516, 2001.

[6] J. Prakash, K. Gururajan: *Effect of velocity slip in an Infinitely Long Rough Porous Journal Bearing,* Tribol. Trans., Vol. 42, No. 3, pp. 661-667, 1999.

[7] K. Vaidyanathan: *Combined Surface Roughness Pattern and Non-Newtonian Effects on the Performance of Dynamically Loaded Journal Bearing,* Tribol. Trans., Vol. 44, No. 3, pp. 428-436, 2002.

[8] D. Zhu, Y.Z. *Ho: Effect of Rough Surface Topography and Orientation on the Characteristics of EHD and Mixed Lubrication in Circular and Elliptical Contacts,* Tribol. Trans., Vol. 44, No. 3, pp. 391-398, 2001.

[9] J.Y. Jang and C.C. Chang: *Adiabatic Analysis of Finite width Journal bearing with Non Newtonian Lubricants,* Wear, Vol. 122, No. 1, pp. 63-75, 1987.

[10] P.C. Mishra, R.K. Pandey, K. Athre: *Temperature Profile of an Elliptic Bore Journal Bearing*, Tribology International, Vol. 40, No. 3, pp. 453-458, 2007.

[11] P.C. Mishra: *Thermal Analysis of Elliptic Bore Journal Bearing*, Tribology Transaction, Vol. 50, No. 1, pp. 137-144, 2007.

[12] P.C. Mishra: *Thermal analysis of elliptic bore journal bearing considering shaft Misalignment*, Tribology Online, Vol. 6, No. 5, pp. 239-246, 2011.

[13] P.C. Mishra: *Mathematical modeling of stability in rough elliptic bore misaligned journal bearing considering thermal and Non-Newtonian effect*, Applied Mathematical modeling, Vol. 37, No. 8, pp. 5896-5912, 2013.

[14] P.C. Mishra: *Modeling for friction of four stroke four cylinder In-Line Petrol Engine,* Tribology in Industry, Vol. 35, No. 1, pp. 74-83, 2013.

NOTATIONS

c	Radial clearance	m
d	Journal diameter	m
e	Eccentricity	
G	Non-circularity coefficient $\left(\frac{\delta-1}{\Psi}\right)$	
h	Film thickness	μm
H	Non-dimensional film thickness	

L	Bearing length	*m*
p	Dimensional pressure	(N/m^2)
P	Non-dimensional pressure $\left(\frac{p\Psi^2}{\eta\omega}\right)$	
Q_{in}	Non-dimensional flow in to the bearing	
Q_s	Non-dimensional side leakages	
r_b	Bearing radius	*m*
r_j	Journal radius	*m*
R *or* Y	Non-dim Roughness parameter	
R_{maj}	Major radius of bearing	*m*
$R_{\min}$	Minor radius of bearing	*m*
T	Dimensional temperature rise	${}^0K$
T_0	Initial temperature of the lubricant.	${}^0K$
U	Journal velocity	*m/sec*
x	Coordinate in the direction of entraining motion	*m*
z	Axial coordinate (direction of side leakage)	*m*
Z	Non-dimensional axial coordinate, $\left(\frac{2z}{l}\right)$	
α	Inclination of major axis with load line	*radian*
$\in$	Eccentricity ratio	
β	Length-diameter ratio	
β_{th}	Thermal coefficient	
δ	Ratio of R_{maj} and $R_{\min}$	
θ	Angular location of the film with respect to load line	*radian*
Ψ	Clearance ratio $\left(c/R_{maj}\right)$	
ϕ	Attitude angle	*radian*
ω	Angular velocity	*rad/sec*
λ	Non-dimensional temperature $\left\{\beta_{th}\left(T-T_0\right)\right\}$	